Journal of Optoelectronics and Advanced Materials Vol. 7, No. 4, August 2005, p. 2029 - 2034

FULLERENE AND NANOTUBES BASED ON ARSENIC NETWORKS. A MODELLING STUDY

S. Zamfira, M. Popescu[a*], F. Sava[a]

"Transilvania"University of Brasov, Faculty of Mechanical Engineering, Precision Mechanics and Mechatronics Department, Brasov, Romania
[a]National Institute of Materials Physics, Bucharest-Magurele, P. O. Box MG. 7, Romania

Arsenic is the main component of many chalcogenide glasses. Due to its triple co-ordination arsenic has the tendency to form two-dimensional networks in both crystalline and amorphous state. Besides the layered form of arsenic it exists molecular arsenic. Small molecules are characteristic to this form of arsenic. Large arsenic clusters have been not identified up to now in amorphous films. A modelling study was carried out in order to demonstrate the possibility to find or to prepare fullerene-like configurations based on arsenic as well as nanotubes (or nanowires) of various diameters.

(Received June 14, 2005; accepted July 21, 2005)

Keywords: Arsenic, Fullerene, Nanotube, Modelling

1. Introduction

Special clusters in low-dimensional system have been discovered as early as 1974. De Neufville, Moss and Ovshinsky [1] were the first who suggested that a freshly evaporated film of As_2S_3 was in fact molecular glass composed of "hard sphere" As_2S_3 molecules. When heated or illuminated the film polymerise or cross-link to form a network structure characteristic of bulk glass. Weiqing Zhou, Paesler and Sayers [2] have shown by X-ray absorption fine structure measurements that films prepared by flash evaporation from As_4S_4 source material have, as a basic component, the cage like As_4S_4 molecule. The molecules are packed in a disordered way as compared to those of crystalline As_4S_4 (realgar).

An important discovery in the low-dimensional systems was the fullerenes [3] based on graphite-like carbon. The C_{60} molecules and their packing in solid structures enriched the chemistry and physics of the carbon and carbon based structures. Later, other types of structures have been discovered: carbon nano-tubes of various diameter [4], multi-wall nanotubes, and onion-like carbon [5].

These discoveries led to the suggestion that other low-dimensional covalent systems, as e.g. chalcogenides could present special configurations similar to fullerenes or nanotubes. Fullerene-like and nanotubes with or without closed ends have been simulated in order to demonstrate that special "objects" are possible at least in arsenic chalcogenides [6]. The self-organisation in arsenic chalcogenides was suggested in [7]. This phenomenon is basically for the formation of the low dimensional objects in chalcogenides [8, 9]. The void structure of tetrahedral material was carefully analysed in [10]. The void-type structure is the feature that induces complex configurations in covalent materials. On the other hand we have carefully modelled the fullerene and nanotube carbon and their interactions [11].

In this paper we try to show that arsenic atoms could be arranged in special configurations as fullerene or small diameter tubes, that respect the crystallochemical requirements of this element, i.e. correct bonding distance and narrow distribution of the bonding angle around the crystallographic bonding angle. Various models have been built and relaxed by computer and the most stable configurations have been pointed out.

* Corresponding author: mpopescu@infim.ro

2. Modelling

At first, a cage-like model of arsenic was built on the schema of fullerene (60 atoms). The model was relaxed by computer. The structure of minimum free energy has been calculated by an iteration procedure based on Monte Carlo – Metropolis method [12] by using the rule of minimisation of the distortion energy for the whole model. The free energy was calculated with the use of force constants taken from the literature, for the bond stretching force constants between two arsenic atoms. The bond stretching potential centred on the As-As bonding distance (r_o=2.51 Å) was taken as $V_1 = A(r^2-r_o^2)$ with $A = 2.4 \times 10^{-5}$ dyn/Å^3 and the bond bending potential centred on the mean equilibrium angle (α=98^o) was taken as $V_2= \beta(\alpha- \alpha_o)^2$ with $\beta = 2.04 \times 10^{-4}$ dyn.Å/rad. The bond stretching force constant of arsenic, determined by J. M. Tranqada and C. Y. Yang [13] from EXAFS measurements in arsenic and arsenic compounds, is situated intermediary between the value for As_2S_3 and that for As_2Se_3. For comparison: the force constant is 1.40×10^{-5} dyn/cm^2 for As_2S_3, 1.14×10^{-5} dyn/cm^2 for As_2Se_3 and 1.20×10^{-5} dyn/cm^2 for arsenic.

Several nanotubes have been built and relaxed by computer-assisted Monte Carlo-Metropolis procedure. The tubes are of different diameters and of different number of atoms. The narrowest tube has 54 atoms, the intermediary one has 72 atoms and the largest one has 100 arsenic atoms.

The number of iterations necessary to reach the minimum free energy in every model depends on the size of the model. As an average, the number of iterations per atom is situated around one million, the step of simulation being variable (from 0.1 Å for the first iteration down to less than 0.000001 Å for the last iterations).

The same nanotubular models have been used to simulate the silicon nanowires. A comparison between the two types of models (for arsenic and for silicon) is given in the next section.

3. Results

The relaxed models of fullerene-like arsenic and nanotube arsenic have been analysed. The bonding distance distributions as well as bond angle and dihedral angle distributions in the models have been calculated. The mean bonding distance, mean bonding angle and the widths of the distributions of distances and angles were calculated. The histograms of the pair distances in the relaxed models have been computed.

Fig. 1 shows the atomic configurations in carbon fullerene and in arsenic fullerene. The size of the arsenic fullerene looks different from the carbon fullerene because the bonding distance for carbon is 1.35 Å, while for arsenic is 2.51 Å.

Fig. 1. The atomic-scale structure of the relaxed arsenic fullerene (a) compared to the relaxed carbon fullerene, C_{60} (b).

Fig. 2 shows the calculated structure factor, bond angle distribution and atom pair distance distribution in arsenic fullerene (a) and in carbon fullerene (b).

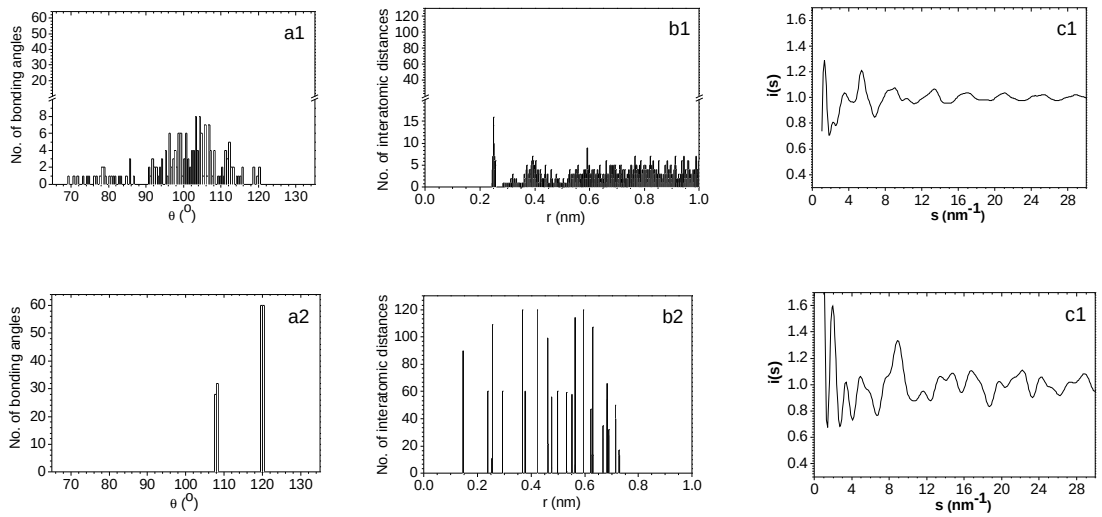

Fig. 2. The structural characteristics of the arsenic fullerene (1) compared to carbon fullerene (2): a. bond angle distribution; b. atom pair distance distribution; c. structure factor.

The arsenic fullerene is different from the carbon fullerene. The orientation of the arsenic bonds alternates with the blind part situated either inside or outside of the cage. Due to the presence of five-fold rings it is not possible to get a perfect alternation. The minimum free energy is 1.73×10^{-3} dyn.Å compared with 0.661×10^{-3} dyn.Å for carbon fullerene. The average bonding angle in arsenic fullerene is shifted from the ideal one (98°) to the value of 103°. A special group of angles are situated in the range 69-87 °. As concerning the pair distribution function the main peaks are well expressed. Nevertheless, a group of distances different from the first and second order distances between atoms, is scattered in a wide range (2.8 – 3.5 Å) at around mid distance between the first and second peak in pair distribution histogram. This means that arsenic fullerene is deformed if compared to carbon fullerene of globular shape. A clear difference between carbon fullerene and arsenic fullerene could be followed in the structure factor. A characteristic of the structure factor in arsenic fullerene is the appearance of a well-expressed first sharp diffraction peak at around 0.35 $Å^{-1}$. The As-As distance is centred on 2.50 Å.

The relaxed arsenic nanotube series is represented in Fig. 3. The diameters of the three nanotubes are: 5.0 Å, 7.0 Å, 8.1 Å. It is interesting to remark that the nanotube with small diameter exhibits a perfect tube shape, while the other nanotubes are distorted. The medium diameter tube is inflated in the middle part, while the large diameter tube is thinner in the middle part and a little bit curved. These specific deformations accomodate the arsenic atoms with low bonding angles, approaching 90 ° when the atoms are forced to take a tube-like geometry.

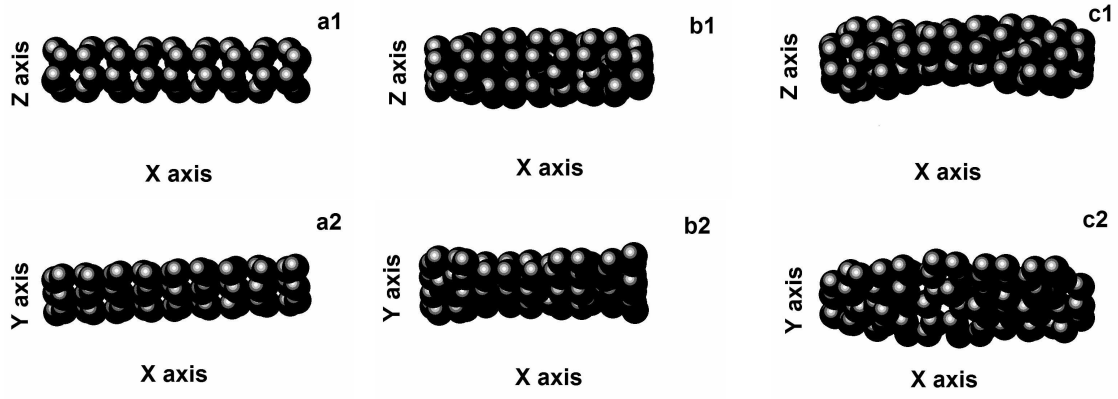

Fig. 3. Arsenic nanotube series: a1, a2. small nanotube (54 atoms). b1, b2. medium nanotube (72 atoms), c1, c2. large nanotube (100 atoms).

In order to have a deeper insight into the structure of nanotubes objects we put in parallel, for comparison, the results obtained on arsenic with the results obtained by simulating, in the same topology, a similar series of silicon nanotubes. Figs. 4-6 show the bond angle distribution, the pair distribution histogram and the structure factor of the arsenic nanotubes compared to silicon nanotubes.

The small diameter arsenic nanotube As_{54} exhibits a distribution of the angles between the bonds situated in the range 104÷115 °. The mean angle is 107.93 °. It is remarkable that the topology of the tube does not allow for respecting the equilibrium angle of arsenic: 98 °, used in relaxation. The relaxed silicon nanotube of the same topology shows a perfect tetrahedral angle, specific to silicon atoms.

The atom pair distribution function (PDF) in small diameter tube As_{54} shows two narrow group of distances that corresponds well to the first peaks in the radial distribution function of amorphous arsenic. The PDF is similar to that of silicon nanotube.

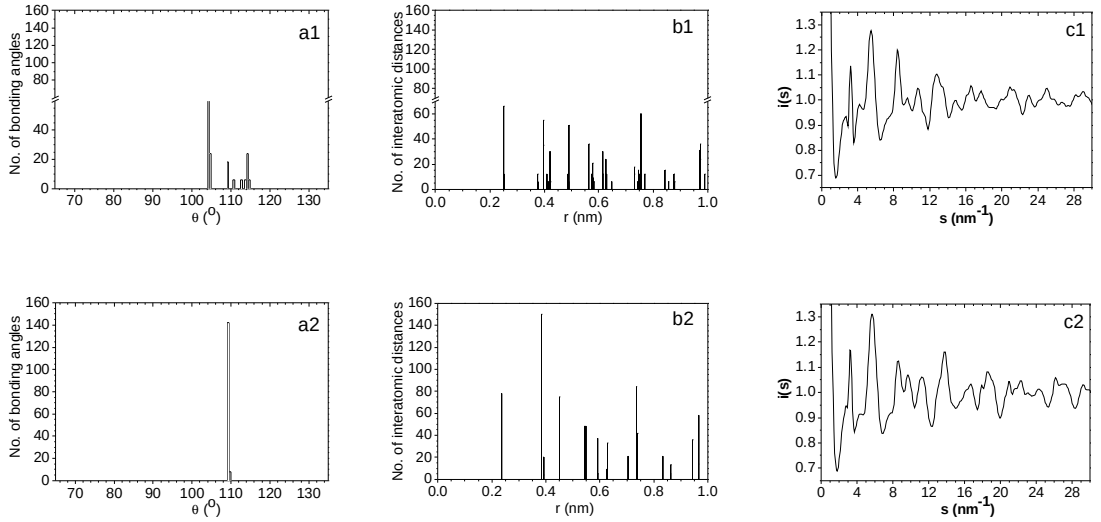

Fig. 4. The structural characteristics of the arsenic nanotubes As_{54} (1) (free energy = 1.3345×10^{-3} dyn.Å) compared to silicon nanotubes Si_{54} (2) (free energy = 4.245×10^{-9} dyn.Å): a. bond angle distribution; b. atom pair distance distribution; c. structure factor.

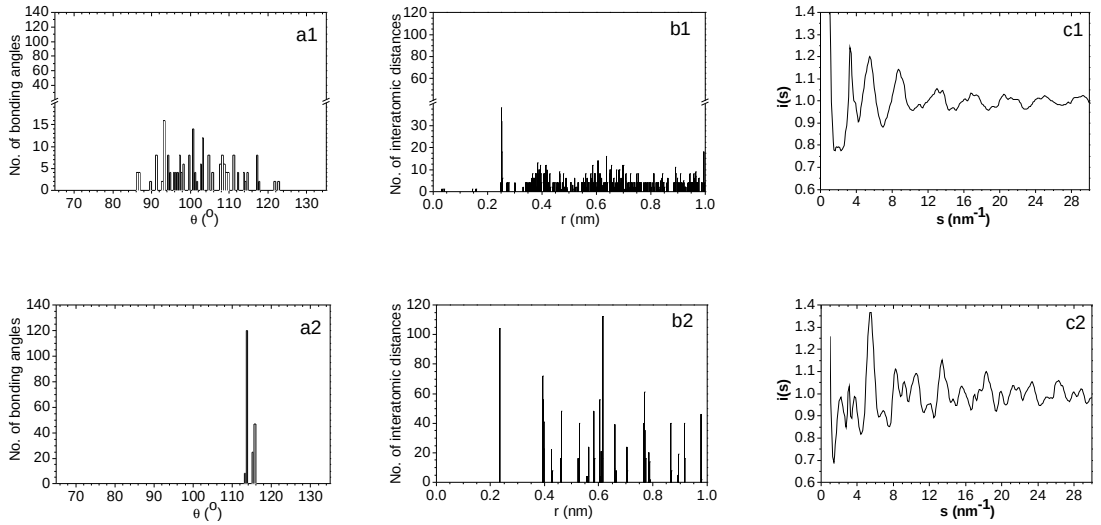

Fig. 5. The structural characteristics of the arsenic nanotubes As_{72} (1) (free energy = 1.3849 $\times 10^{-3}$ dyn.Å) compared to silicon nanotubes Si_{72} (2) (free energy = 3.723×10^{-4} dyn.Å): a. bond angle distribution; b. atom pair distance distribution; c. structure factor.

The medium diameter arsenic nanotube As_{72}, exhibits a bonding angle distribution in the range 86÷123 °. The average bond angle is 102.2 °. This value demonstrates that the arsenic-bonding angle is maintained but significant fluctuations of its value appear. In the corresponding silicon nanotube, the tetrahedral angle is not 109.5°, as in normal silicon bond, but is shifted to 114.33 °.

In medium size nanotube As_{72}, the peaks of the PDF are enlarged, showing a disorder due to bond angle fluctuations.

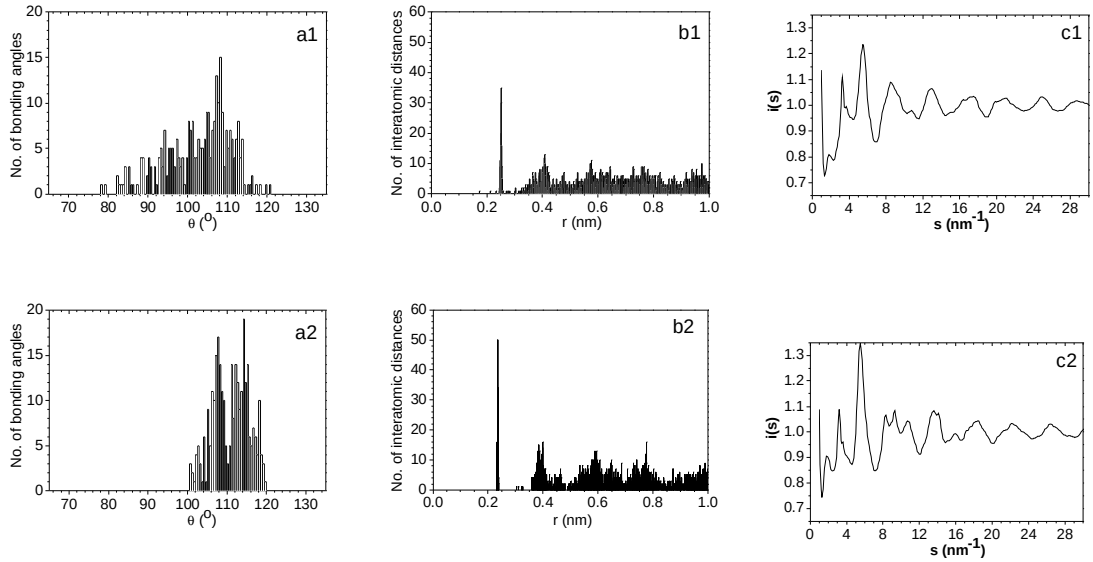

Fig. 6. The structural characteristics of the arsenic nanotubes As_{100} (1) (free energy = 2.1539 $\times 10^{-3}$ dyn.Å) compared to silicon nanotubes Si_{100} (2) (free energy = 5.6015×10^{-4} dyn.Å): a. bond angle distribution; b. atom pair distance distribution; c. structure factor.

The nanotube with largest diameter, As_{100}, exhibits a large bond angle distribution. The mean angle is 102.61°. A long tail towards small angles is specific to this tube. The tendency towards splitting of the angles in higher bond angles and lower angles is, of course, due to the topology of the nanotube. The output is the distortion of tube symmetry, as seen in Fig. 3.

In large-size nanotube the PDF exhibits much larger peaks. In both medium and large nanotubes, a group of several distances are situated in-between the first neighbour peak and second neighbour peak, this speaking in favour of a significant distortion occurring in nano-tubes during relaxation. It is remarkable that similar distances (only four distances) are characteristic to the large size silicon nanotube.

The structure factor of arsenic nanotubes shows a first peak situated at 0.2573 $Å^{-1}$ for As_{54}, 0.1902 $Å^{-1}$ for As_{72}, and 0.1839 $Å^{-1}$ for As_{100}. These peaks correspond to the quasi-distances of 3.886 Å, 5.258 Å and 5.438 Å, respectively. The silicon nanotubes exhibit also a narrow first peak. It is remarkable that instead of this peak the medium size tube exhibits a group of small peaks (three).

Finally we must observe that the free energy of the models (the total distortion energy) is very different. The minimum distortion energy (E = 1.33×10^{-3} dyn.Å) was obtained for the small diameter model of arsenic.

4. Discussion

The arsenic fullerene is possible to be built, but the distortions of the bonds (angle bonds) are enough large. Other configurations based on closed cluster with a different topology of rings of arsenic must be proved by simulation. It is possible that a six fold rings topology of fullerene and

alternated orientation of the arsenic blind part, will allow for a more regular configuration and a better fitting with the bond angle of arsenic.

Nanotubes based on arsenic are possible. The total free energy in the models shows that the most stable configuration is that of small size nanotube.

There are a lot of amorphous materials based on arsenic. They are characterised by photostructural transformations, an important phenomenon for applications [14-27]. The underconstrained or over constrained networks are able to transforms under the influence of external factors. It is possible that the distorted arsenic networks characteristic to arsenic fullerene or nanotube arsenic become metastable and easily transformable under the action of specific external factors: heat, pressure, light... The transformation is accompanied by change of optical transparency due to the shift of the absorption edge. That is why the study and a possible preparation of the low-dimensional objects are important.

5. Conclusions

We have demonstrated that several special nano-configurations of arsenic are possible, although with some distortion of the ideal bonding of arsenic atoms. Arsenic fullerene and small arsenic nanotubes exhibit low distortion energies and, therefore, they are good candidates for metastable low-dimensional configurations of arsenic.

Work is in progress to find other more stable configurations of arsenic characterised by different topologies and lower distortion energy of the bonds. Such metastable configurations could be proposed for preparation, or for identification in amorphous arsenic.

References

[1] J. P. De Neufville, S. C. Moss, S. R. Ovshinsky, J. Non-Cryst. Solids **13**, 191 (1974).
[2] Weiqing Zhou, M. A. Paesler, D. A. Sayers, Phys. Rev. D, **43**, 11920 (1991).
[3] H. W. Kroto, J. R. Heath, S. C. O'Brien, R. F. Curl, R. E. Smalley, Nature, **318**, 162 (1985).
[4] S. Iijima, Nature, **354**, 56 (1991).
[5] D. Ugarte, Nature, **359**, 707 (1992).
[6] A. Lorinczi, M. Popescu, F. Sava, J. Optoelectron. Adv. Mater. **6**(2), 489 (2004).
[7] M. Popescu, J. Optoelectron. Adv. Mater. **5**(5), 1059 (2003).
[8] M. Popescu, F. Sava, A. Lorinczi, J. Optoelectron. Adv. Mater. **6**(3), 887 (2004).
[9] M. Popescu, J. Optoelectron. Adv. Mater. **6**(4), 1147 (2004).
[10] F. Sava, J. Optoelectron. Adv. Mater. **5**(5), 1075 (2003).
[11] A. Lorinczi, M. Popescu, F. Sava, A. Anghel, J. Optoelectron. Adv. Mater. **6**(1), 349 (2004).
[12] M. Popescu, Ph. D. Thesis, 1975, Central Institute of Physics, Bucharest, Romania.
[13] J. M. Tranqada, C. Y. Yang, private communication
[14] H. Jain, J. Optoelectron. Adv. Mater. **5**(1), 5 (2003).
[15] D. Lezal, J. Optoelectron. Adv. Mater. **5**(1), 23 (2003).
[16] M. Stabl, L. Tichy, J. Optoelectron. Adv. Mater. **5**(2), 429 (2003).
[17] I. Ohlidal, D. Franta, M. Frumar, J. Jedelesky, J. Omasta, J. Optoelectron. Adv. Mater. **6**(1), 139 (2004).
[18] M. Stabl, L. Tichy, J. Optoelectron. Adv. Mater. **6**(3), 781 (2004)
[19] K. Tanaka, T. Gotoh, K. Sugawara, J. Optoelectron. Adv. Mater. **6**(4), 1133 (2004).
[20] J. Dikova, Tz. Babeva, P. Sharlandiev, J. Optoelectron. Adv. Mater. **7**(1), 361 (2005).
[21] A. A. Babaev, I. K. Kamilov, A. M. Askhabov, S. B. Sultanov, J. Optoelectron. Adv. Mater. **5**(5), 1231 (2003).
[22] J. Teteris, M. Reinfelde, J. Optoelectron. Adv. Mater. **5**(5), 1355 (2003).
[23] D. Lezal, J. Pedlikova, J. Zavadil, J. Optoelectron. Adv. Mater. **6**(1), 133 (2004).
[24] P. Sharlandiev, B. Markova, J. Optoelectron. Adv. Mater. **5**(1), 39 (2003).
[25] Ke. Tanaka, T. Gotoh, K. Sugawara, J. Optoelectron. Adv. Mater. **6**(4), 1133 (2004).
[26] M. L. Trunov, V. S. Bilanich, J. Optoelectron. Adv. Mater. **5**(5), 1085 (2003).
[27] M. L. Trunov, V. S. Bilanich, J. Optoelectron. Adv. Mater. **6**(1), 157 (2004).